

# Automatic generation of Regions Of Interest for Radionuclide Renograms

David C Barber

Department of Medical Imaging and Medical Physics  
Central Sheffield Teaching Hospitals, Glossop Road, Sheffield S10 2JF

**Abstract.** Automatic generation of kidney regions of interest for radionuclide renograms is possible by defining a reference image and reference regions, using a non-linear image registration algorithm to map a totalised image from a patient to the reference image and using the mapping produced to map the predefined reference regions back onto the patient image. The accuracy of the automatically derived regions is evaluated by comparison with regions drawn independently by experienced operators. The median success factors, a measure of the overlap between automatic and manual regions, over 49 kidneys was 0.95 and the average linear displacement between the boundaries of the automatic and manual regions was 0.43 in units of pixel dimensions.

## 1 Introduction

One of the principal uses of image segmentation, in terms of the number of patients involved, is the use of regions-of-interest (ROI) in Nuclear Medicine. These are invariably drawn manually, although there is evidence that ROI drawn on the same subject can be quite operator dependent. White et al [1] compared two operator drawn regions of interest using a success factor, defined as the area of the intersection of the regions divided by the average area of the regions and obtained intra-operator variability of 0.94 and inter-operator variability of 0.93. A reliable and automatic method of drawing ROI would be useful clinically and would help to standardise analysis between clinics. In the analysis of radionuclide renograms an ROI is drawn around each kidney to allow the total activity in the kidney to be estimated as a function of time. Background regions, often automatically derived from the kidney regions, are drawn to allow background subtraction. In spite of the widespread use of ROI analysis in clinical practice in Nuclear Medicine there is still no general method of drawing ROI automatically. The images are low resolution compared to many other modalities and are noisy, both of which makes identification and delineation of edges difficult. Other approaches to renogram analysis using factor analysis have been explored. The aim of this approach is to extract curves representing the variation in activity with time in various homogeneous structure in the study, such as the kidney and bladder, from a low dimensional factor space derived from the study. Although extensively researched there is little evidence that these techniques have made much impact clinically. Indeed Martel [2] showed that there was little gain over using optimal ROI. Jose [3] has proposed a method for generation of ROI for kidneys which uses a combination of dynamic information, multi-level intensity segmentation, neural network identification of segments associated with the kidneys and morphological operations to generate kidney ROIs. However, this approach is specific to kidneys and as far as we are aware has not been extended to other areas of the body. Jose [3] reports median success factors of 0.9 for a 30 renogram clinical test set.

In this paper we propose the use of image registration to generate reliable and robust ROI for radionuclide renograms. Houston et al [4] described the use of image registration to generate automatic ROI for cardiac studies using an affine transform. However, the affine transform is in general too restrictive and non-linear transforms are required. ROI generation using registration is generic, in the sense that the domain knowledge is completely separated from the algorithm and trainable, in the sense that exemplar data can be used to define how the ROI is drawn. It does not rely on any assumptions about organ boundaries being defined by appropriate intensity levels or gradient values.

## 2 Theory

The aim of registration is to map an image  $m(x,y)$ , the moved image, to an image  $f(x,y)$ , the fixed image. We assume that such a mapping is possible in that there is a one-to-one mapping which converts  $m(x,y)$  to  $f(x,y)$  such that the intensity values completely match (in the absence of noise). Then the moved and fixed images can be related by

$$m(x + \Delta x(x, y), y + \Delta y(x, y)) = f(x, y)$$

where  $\Delta x(x,y)$  and  $\Delta y(x,y)$  together constitute the mapping function.

In the current work we modify equation (1) by adding an extra term

$$m(x + \Delta x(x, y), y + \Delta y(x, y)) - \Delta s(x, y) = f(x, y) \quad (1)$$

which deals with the residual differences between the two images. In this form, the mapping function (including the  $\Delta s(x, y)$  term) is clearly non-unique. However, if smoothness constraints are imposed on the mapping functions unique solutions are possible. One such constraint is to expand the mapping functions in terms of a set of basis functions  $\phi_i(x, y)$ . We can show that, for images close together

$$f(x, y, z) - m(x, y, z) = \frac{1}{2} \Delta x(x, y) \left[ \frac{\partial f}{\partial x} + \frac{\partial m}{\partial x} \right] + \frac{1}{2} \Delta y(x, y) \left[ \frac{\partial f}{\partial y} + \frac{\partial m}{\partial y} \right] - \Delta s(x, y) \quad (2)$$

and if the mapping function is expanded in terms of the basis functions

$$f(x, y) - m(x, y) = \frac{1}{2} \sum_{\text{all } i} a_{xi} \phi_i(x, y) \left[ \frac{\partial f}{\partial x} + \frac{\partial m}{\partial x} \right] + \frac{1}{2} \sum_{\text{all } i} a_{yi} \phi_i(x, y) \left[ \frac{\partial f}{\partial y} + \frac{\partial m}{\partial y} \right] - \sum_{\text{all } i} a_{si} \phi_i(x, y)$$

where each of the summations is a component of the mapping function expanded in terms of the basis functions and this equation can be written in vector matrix form as

$$\mathbf{f} - \mathbf{m} = \mathbf{T}\mathbf{a}$$

where  $\mathbf{a}$  is a vector of the coefficients of the basis function expansions of the mapping functions. Provided the number of pixels is greater than the number of elements in  $\mathbf{a}$ , we have an over-determined set of equations and can solve for the elements of  $\mathbf{a}$  and hence obtain the mapping.

Simple linear basis functions define an affine mapping. In the present work local (bilinear) basis functions are used. In this case the elements of  $\mathbf{a}$  represent the mapping values at points on a grid defined by the central points of the local basis functions. We can sensibly apply additional smoothness constraints to the values in  $\mathbf{a}$ . Computation of  $\mathbf{a}$  is an iterative (gradient descent) process. If  $\mathbf{a}_n$  is the current estimate of  $\mathbf{a}$  the next increment  $\Delta \mathbf{a}$  is given by

$$\Delta \mathbf{a} = [\mathbf{T}^t \mathbf{T}(\beta) + \lambda \mathbf{L}^t \mathbf{L}]^{-1} (\mathbf{T}^t (\mathbf{f} - \mathbf{m}(\mathbf{a}_n)) - \lambda \mathbf{L}^t \mathbf{L} \mathbf{a}_n)$$

where  $\lambda$  is a parameter controlling the overall force of the smoothing constraint,  $\beta$  is a separate and independent parameter controlling the relative importance of the amplitude term compared to the spatial terms and  $\mathbf{L}$  is a Laplacian operator.  $[\mathbf{T}^t \mathbf{T}(\beta) + \lambda \mathbf{L}^t \mathbf{L}]$  is a sparse matrix and the above equation can be solved very efficiently using gradient descent methods.

Inclusion of the  $\Delta s(x, y)$  in equation 1 without constraint results in a trivial solution in that  $\Delta s(x, y)$  can be set to  $f - m$ . However, consider equation 2. The difference between  $f$  and  $m$  is made up of contributions from three terms. If each of these terms contributes equal amounts to the differences between  $f$  and  $m$  then since the gradients are relatively non-smooth functions  $\Delta x$  and  $\Delta y$  will be smoother than  $\Delta s$ . The *smoothest* way of accounting for the difference between  $f$  and  $m$  is as far as possible to utilise the first two terms and then evoke  $\Delta s$  when all else fails. The total smoothing value is given by

$$\mathbf{L}(\Delta x) + \mathbf{L}(\Delta y) + \beta \mathbf{L}(\Delta s)$$

where  $\beta$  controls the relative importance of the smoothness of the spatial and intensity mappings. Values of  $\lambda$  and  $\beta$  can be found which minimise the condition number of  $[\mathbf{T}^t \mathbf{T}(\beta) + \lambda \mathbf{L}^t \mathbf{L}]$  and these are the values used in this work.

The mapping functions are computed using image data within a registration region around the kidneys.

### 3 Methods

A renogram consists of a sequence of gamma camera images which follow the passage of a radiotracer through the kidneys. In our clinic the initial phase of the study consists of 20 images each of 2 seconds duration to capture the vascular phase of the investigation and then a second phase consisting of a further 70 or so images each of 20 seconds duration. The ROI are generated using the first 10 images of the second component. These are summed together and (apart from the vascular phase) represent approximately the first three minutes of the study. The activity in the kidney is normally increasing over this phase of the study and the totalised images show, when there is uptake, both kidneys. A summed image from a normal study is taken as the starting point and a set of normal patient images registered to this image. The average of these registered images is computed, and this becomes the temporary reference image. The set of images is now registered to this temporary reference and the again the average of the registered images is computed. This image forms the reference image. The reference image used in this study is shown in Figure 1, along with the rectangular registration region used.

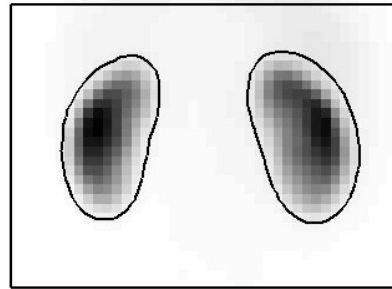


Figure 1. The reference image, the reference regions and the registration region.

Regions of interest around the kidney are drawn for each of the normal images. The regions used in this study were those produced during routine clinical analysis and have been drawn by a variety of users. The ROI can be in two forms. The first is as a vector of boundary points and the second is as a binary image. To generate a reference ROI each normal image is registered to the reference image and the same mapping is then applied to the corresponding ROI in binary form. All the registered binary ROI are then averaged, the average converted to binary form using a 50% threshold and then converted to vector form using a contour following algorithm. The resulting reference region is also shown in Figure 1.

To generate an ROI automatically for a new patient the patient image is registered to the reference image, and then the mapping used to map the reference ROI back to the patient image. In this work an initial registration of patient image to standard image was performed. This was then followed by a registration of each kidney separately to the corresponding reference. Computation time for generation of the automatic regions was under 0.5 seconds per study.

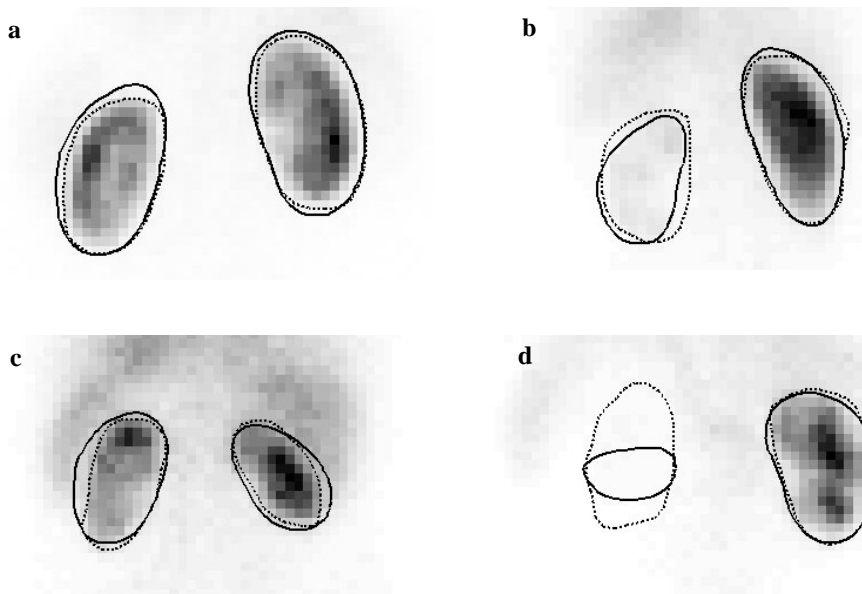


Figure 2. Four studies from the set of 25. See text for details.

The reference image and region were generated using data from 25 normal images. The method was evaluated using an additional 25 subjects, which included a mixture of 6 subjects with visually normal patterns of uptake and 19 subjects with abnormal patterns of uptake (including one study with a non-visualised kidney). The automatically generated regions were compared to the manual regions by dividing the area of the intersection of the two regions by the average area of the two regions. The ratio is the success factor (SF). If the regions completely overlap the value of this measure is 1, if they do not overlap at all the value of this measure is zero. A second measure of the overlap of the manual and automatic regions was obtained by dividing the area of the exclusive or of the two regions by the average of the perimeter of the regions. This length, in units of pixels, is a measure of the average linear displacement (ALD) between the two boundaries.

## 4 Results

Figure 2 shows four studies from the 25. The solid contours represent the automatically generated ROI, the dotted contours the manually generated contours. Figure 2a has the largest success factor averaged over both kidneys (SF = 0.97). Figures 2b and 2c show the worst cases from this data set. Figure 2b has very poor function in the left kidney (SF = 0.84 for the left kidney), and Figure 2c shows a study with overall reduced function in both kidneys (SF = 0.86 and 0.87 for the left and right kidneys). Figure 2d shows a study with a completely non-functioning kidney. The median SF was 0.95 over all kidneys (excluding the non-visualised kidney). The smallest value corresponds to the left kidney region in Figure 2d. The next smallest value corresponds to the left kidney in Figure 2c. The median ALD, again excluding the non-visualised kidney, was 0.43 pixels.

## 5 Discussion

This method for generating automatic ROI required no manual intervention, which made it a fully automatic method. Jose [3], using a combination of dynamic information, multi-level intensity segmentation, neural networks for segment identification and morphological operators, achieved a median SF of 0.9 over both kidneys (excluding dramatic failures). In the present work the reference image and the reference ROI are generated by a process of training with exemplars. In the present case the exemplars are the ROI generated by manual operation. We do not know if these are the best that can be produced, but clearly if a better set of ROI can be produced they can form the basis of a training set.

The cost function minimised is a sum-of-squares cost function, modified to include an amplitude term. Use of this function is limited to registering images of the same modality. Although less general than methods based on information theoretic measures the approach described in this paper does have the advantage of computational efficiency and robustness which means that it can be operated unsupervised in a clinical environment. We have deliberately not used any dynamic information in this work, but clearly images could be produced which combined both spatial and dynamic information (for example parametric images of temporal gradient) and these may produce even better results. However, in its present form the method is generic in that the domain knowledge (reference data) is separated from the computational component of the method. The same approach has been used (Barber [5]) to segment MUGA images, with a reported SF of 0.93, so the method looks promising for the generation of ROI for dynamic nuclear medicine studies.

## 6 Conclusion

Automatic and reliable generation of kidney regions of interest on radionuclide renograms in a clinically useful timescale is possible.

## References

1. D D R White, A S Houston, W F D Sampson and G P Wilkins. Intra- and interoperator variations in region-of-interest drawing and their effect on the measurement of glomerular filtration rates. *Clinical Nuclear Medicine* 24(3):117-181 1999
2. A L Martel. The use of factor methods in the analysis of dynamic Radionuclide studies. PhD thesis, University of Sheffield, 1992
3. R M J Jose. Analysis of Renal Nuclear medicine Images. PhD Thesis University of London 2000
4. A S Houston, D White, W F D Sampson, M Mcleod and J Pilkington. An assessment of two methods for generation automatic regions of interest. *Nucl. Med. Commun.* 19:1005-1016 1998.
5. D C Barber Automatic ROI generation using image registration (abs). *Nucl Med. Commun.* 23, Oct 2002